Energy Proceedings
Vol 29, 2022
ISSN 2004-2965

Heat and mass transfer of biomass particles under acoustic oscillation fields[#]

Diego Neves Kalatalo[1], Andrew Cantanhede Cardoso[1], Jackson Costa da Silva[1], Luiz Alberto Baptista Pinto Júnior[1], Pedro de França Santos[1], Rogério Luiz Veríssimo Cruz[1], Carlos Alberto Gurgel Veras[2]

1 University of Brasília – Graduate Program in Mechanical Sciences

2 University of Brasília – Energy and Environment Laboratory – LEA/UnB

ABSTRACT

The objective of this work is to study heat and mass transfer processes in a single biomass particle before its thermal degradation (< 200 °C) under high intense acoustic fields. For that, was developed a numerical code for Biot number higher that one, i.e., non-isothermal particles. The hypothesis is that an acoustic field alters the interaction between the gas and particles, proving drying. Acoustic fields can be obtained by using a loudspeaker inside a reactor. The proposed model predicts moisture mass transfer completion for different particle sizes and oscillating frequencies. The obtained data are relevant for plant conversion capacity and reactor's preliminary design.

Keywords: renewable energy resources, numerical predictions, pyrolysis reactor, acoustic oscillations

NOMENCLATURE

Abbreviations	
EES	Engineering Equation Solver
Symbols	
d_p	Particle diameter
m_p	Particle mass
g	Local gravity
F_W	Weight force
F_D	Drag force
C_D	Drag coefficient
ρ_g	Gas density
u_g	Gas velocity
u_p	Particle velocity
u_r	Relative velocity
$\bar{u}_g$	Gas average velocity
$\tilde{u}_g$	Amplitude gas velocity
Re	Reynolds number
μ_g	Gas viscosity
$\dot{m}_g$	Gas mass flow
π	Pi number
d_{pipe}	Pipe diameter
f	frequency
t	Time
a_p	Particle acceleration
u_0	Initial particle velocity
z_0	Initial particle position
z_p	Particle position
n	Number of points along radius
Δr	Finite difference along radius
R	Particle external radius
i	i th element
r	Radius
α	Thermal diffusivity coefficient
T	Temperature
T_0	Initial temperature
k	Thermal conductivity
ρ_p	Particle density
cp_p	Particle specific heat capacity
$\bar{h}$	Convective heat transfer coefficient
T_f	Gas flow bulk temperature
Pr	Prandtl number
cp_g	Gas specific heat capacity
k_g	Gas thermal conductivity
Nu	Nusselt number
X	Moisture concentration
X_f	Gas flow bulk moisture concentration
X_0	Initial moisture concentration
D	Mass diffusivity coefficient
$\bar{h}_m$	Convective mass transfer coefficient
Sc	Schmidt number
Sh	Sherwood number
m_{db}	Dry basis mass
ρ_0	Initial density
v	Volume

1. INTRODUCTION

Despite the economic downturn in 2020 the use of renewable sources continued to grow [1]. At the same time, the use of non-renewable sources is continuously being diminished, due to their depletion [2].

Heat and power generation from biomass is even more relevant nowadays due to scientific and industrial interest regarding to diminishing availability of fossil fuels and its relationship with environment preservation.

In Brazil, waste biomass can be used to produce different types of fuels for heat and power generation. Biomass conversion through pyrolysis produces liquid, solid and gas fuel products, which are easily to burn than the original feedstock. Solid biomass and waste are very difficult and costly to manage which also gives impetus to pyrolysis research [3], [4].

A relatively recent thermochemical technology applied to this field promoted the enhancement of biomass fuel characteristics. This technology is known as torrefaction or mild pyrolysis.

Mild pyrolysis changes the biomass properties resulting in a much better fuel quality for combustion and gasification applications. In addition, it improves the calorific value and grindability.

The proposed modeling for the temperature field in the particle derives from the use of energy equation, which associates time to space variation. In this perspective, residence time is an essential analysis variable.

Biomass residence time increases with decreasing air flowrate and increasing biomass load, but when it increases the biomass weight it also increases the char yield and heat loss during devolatilization. Also, that lows residence time can influence the percentage of unconverted biomass during the gasification time [5], [6]. With acoustic flows it's possible to control the residence time to control the drying and the reactions during the gasification process.

This paper thus presents a numerical model to predict mass and heat transfer processes during single biomass drying under high intensity acoustic fields.

2. MODELLING

2.1 Characterization of biomass

The computational model allows simulations of any type of wood particles, by inserting specific properties as input data. For many species of wood, properties such as moisture content and specific gravity can be found in [7].

The biomass employed in this work was the Pinus Pinaster sawdust with a density of 225 kg/m³ [8] and moisture content of 8.6% [9], which is an extended drying condition.

2.2 Pyrolysis reactor description

A system design is presented in Fig. 1, consisting of a biomass feeder source and a pyrolysis reactor, with biomass' round particles under the influence of a speaker induced oscillation.

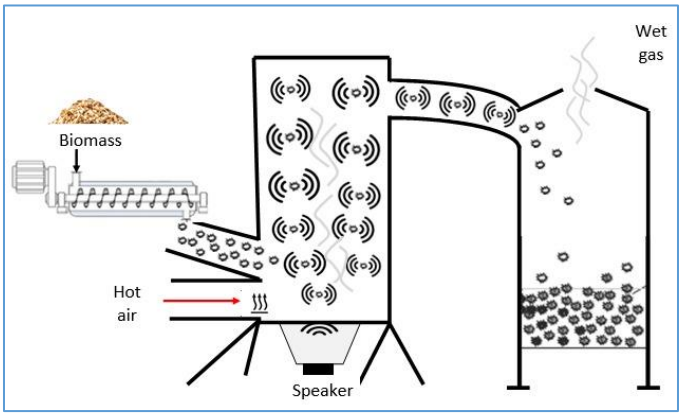

Fig. 1 Pyrolysis reactor under acoustic oscillation given by a speaker (at the center) and storage reservoir (at right).

3. THEORY

3.1 Hydrodynamics, mas and heat transfer

In the model, a biomass particle of diameter d_p, mass m_p and weight F_W flowing under acoustic field, subjected to a drag force F_D.

Weight force is given by $F_W = m_p g$, g is the local gravity. Drag force is given by

$$F_D = \frac{\pi \left(\frac{d_p}{2}\right)^2 C_D \rho_g |u_r| u_r}{2}$$

where C_D is the drag coefficient, taken as a function of the Reynolds number Re, calculated by Equation 1 for a given gas viscosity μ_g.

Gas density is given by ρ_g and the relative velocity u_r between gas and particle velocities u_g and u_p is given by $u_r = u_g - u_p$.

$$Re = \frac{\rho_g |u_r| d_p}{\mu_g} \qquad \text{Equation 1}$$

Gas flow through reactor at an average constant velocity $\bar{u}_g$, determined by Equation 2.

$$\bar{u}_g = \frac{\dot{m}_g}{\pi \left(\frac{d_{pipe}}{2}\right)^2 \rho_g} \qquad \text{Equation 2}$$

Gas mass flow is given by $\dot{m}_g$, considering a cylindrical reactor of diameter d_{pipe}.

Equation 3 [10] insert acoustic field oscillation and calculate gas velocity u_g. The amplitude gas velocity $\tilde{u}_g$ is constant and equals to 10 m/s, u_g varies through time t and oscillation frequency f.

$$u_g = \bar{u}_g + \tilde{u}_g \sin(2\pi f t) \qquad \text{Equation 3}$$

Forces balance between weight and drag results particle's acceleration a_p, as presented at Equation 4.

$$F_W + F_D = m_p a_p \qquad \text{Equation 4}$$

Considering an initial particle's velocity u_0 and particle's acceleration a_p in Equation 5, yields local particle's velocity u_p.

$$u_p = u_0 + \int_0^t a_p dt \qquad \text{Equation 5}$$

Assuming an initial particle's position z_0, the particle position z_p relative to vertical axis is given by Equation 6.

$$z_p = z_0 + \int_0^t u_p dt \qquad \text{Equation 6}$$

Temperature distribution inside the particle is obtained after discretization applying a finite difference method. The particle was divided in a series of control volumes whose radial length is given by

$$\Delta_r = \frac{R}{n-1}$$

, where n is the number of points along the radius R.

Since the domain is divided in $n-1$ elements and $i \in \{1,..,n\}$, for convenience, the notations can be adopted in terms of $(r = 0\ or\ i = 1)\ and\ (r = R\ or\ i = n)$ with no loss of generality.

Space Domain diagram can be geometrically described by Fig. 2.

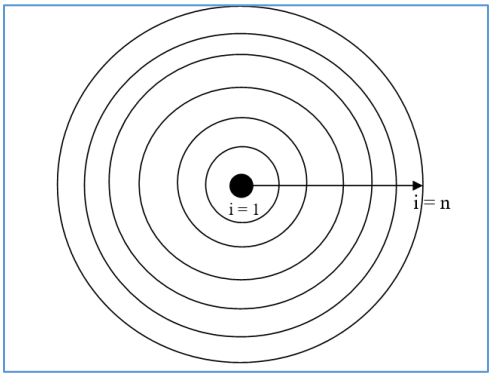

Fig. 2 Biomass particle radial control volumes, likewise onion layers, $i \in \{1,..,n\}$.

THIBAULT et al [11] presented a spherical discretization model for energy equation. Energy equation with no heat generation in spherical coordinates and one dimension is given by Equation 7.

$$\frac{\partial T}{\partial t} = \alpha \frac{1}{r^2} \frac{\partial}{\partial r}\left(r^2 \frac{\partial T}{\partial r}\right) \qquad \text{Equation 7}$$

Thermal diffusivity coefficient α is given by

$$\alpha = \frac{k}{\rho_p c p_p}$$

, where k, ρ_p and cp_p are the particle thermal conductivity, density and specific heat capacity respectively. It was assumed that k and cp_p are functions of T. Empirical correlations from [7] were used to set these properties.

Boundary and initial value conditions are given in Equations 7a, 7b and 7c.

$$\left(\frac{\partial T}{\partial r}\right)_{r=0} = 0 \qquad \text{Equation 7a}$$

In Equation 7a set it is assumed symmetry conditions, then

$$-k_n \left(\frac{\partial T}{\partial r}\right)_{r=R} = \bar{h}\left(T_n - T_f\right) \qquad \text{Equation 7b}$$

Equation 7b set the Robin boundary condition, where convective and conductive heat fluxes sum to zero. T_f is the bulk temperature of gas flow.

$$T(r,0) = T_0 \qquad \text{Equation 7c}$$

Equation 7c set the initial condition, where all the domain is at the initial temperature T_0.

Prandtl, Reynolds and Nusselt number from [12] are applied to calculate the average convective heat transfer coefficient $\bar{h}$. Temperature field is calculated with the help of Equation 11.

$$Pr = \frac{\mu_g c p_g}{k_g} \qquad \text{Equation 8}$$

where gas specific heat capacity is given by cp_g.and gas thermal conductivity is given by k_g.

$$Nu = \frac{\bar{h} d_p}{k_g} \qquad \text{Equation 9}$$

$$Nu = 2 + 0.6 Re^{1/2} Pr^{1/3} \qquad \text{Equation 10}$$

$$T = T_0 + \int_0^t \frac{\partial T}{\partial t} dt \qquad \text{Equation 11}$$

Drying is calculated by the moisture concentration decrease in particle (X). Second order Fick's law equation in axisymmetric spherical coordinates is given by Equation 12.

$$\frac{\partial X}{\partial t} = D \frac{1}{r^2} \frac{\partial}{\partial r}\left(r^2 \frac{\partial X}{\partial r}\right) \qquad \text{Equation 12}$$

Mass diffusivity coefficient D is assumed as function of T. Therefore, were adopted empirical correlation from [13] to this property.

Boundary and initial value conditions are given by Equations 12a, 12b and 12c.

$$\left(\frac{\partial X}{\partial r}\right)_{r=0} = 0 \qquad \text{Equation 12a}$$

$$-D_n\left(\frac{\partial X}{\partial r}\right)_{r=R} = \bar{h}_m\left(X_n - X_f\right) \qquad \text{Equation 12b}$$

Equation 12b set the Robin boundary condition, where convective and diffusive mass fluxes sum to zero. X_f is the bulk moisture concentration of the gas flow.

$$X(r,0) = X_0 \qquad \text{Equation 12c}$$

Equation 12c set the initial condition, where all the solid domain is at the initial moisture concentration X_0.

Schmidt, Reynolds and Sherwood number from [12] in Equation 15 are applied to calculate the average convective mass transfer coefficient $\bar{h}_m$.

$$Sc = \frac{\mu_g}{\rho_g D_n} \qquad \text{Equation 13}$$

$$Sh = \frac{\bar{h}_m}{\frac{D_n}{d_p}} \qquad \text{Equation 14}$$

$$Sh = 2 + 0.6Re^{1/2}Sc^{1/3} \qquad \text{Equation 15}$$

Moisture concentration field is calculated by Equation 16.

$$X = X_0 + \int_0^t \frac{\partial X}{\partial t}dt \qquad \text{Equation 16}$$

Mass variation due to drying particles is modelled by equations 17, 18 and 19.

$$m_{db_i} = \left(\frac{\rho_0}{1+X_0}\right)v_i \qquad \text{Equation 17}$$

$$\frac{dm_i}{dt} = m_{db_i}\frac{dX_i}{dt} \qquad \text{Equation 18}$$

$$m_i = \rho_0 v_i + \int_0^t \frac{dm_i}{dt}dt \qquad \text{Equation 19}$$

Particle mass m_p at each time t is calculated by Equation 20.

$$m_p = \sum_{i=2}^{n} m_i \qquad \text{Equation 20}$$

4. RESULTS AND DISCUSSION

4.1 Numerical solution and validation model

The derived differential equations are solved numerically using the equation-based integral function of the Engineering Equation Solver platform [14].

Two grid points with 10 and 100 control volumes were employed to check system sensitivity for grid sizing. Since the numerical results were very similar, the code was deemed adequate for further particle drying analysis.

The discretized method was also compared with EES library function from an analytical solution [15] resulting differences between numerical and analytical solution results lower than 5.0E-4 K.

Drying of 0.1 to 10 mm particle diameter was then simulated under pulsating flow. Fig. 5b and Fig. 5d shows that the heat and mass transfer coefficients $\bar{h}$ and $\bar{h}_m$ are higher than those without the oscillation, as shown in Fig. 5a and 5c.

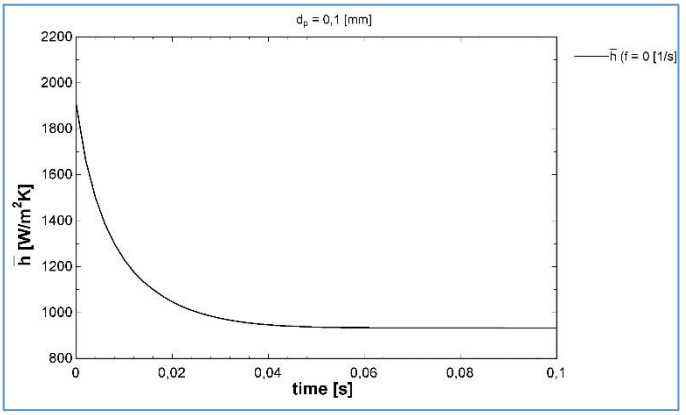

Fig. 5a: Heat transfer coefficient under steady flow.

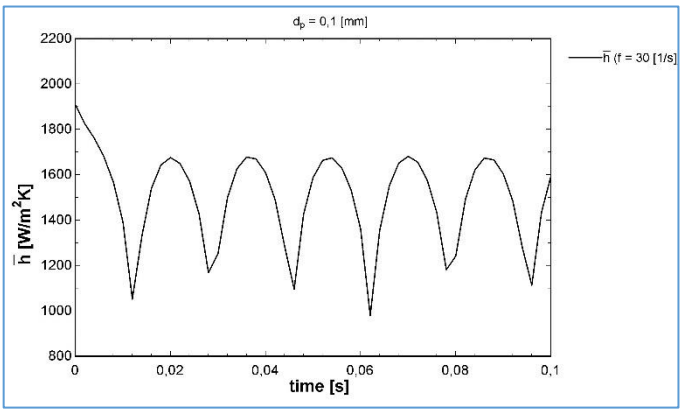

Fig. 5b: Heat transfer coefficient under pulsating flow.

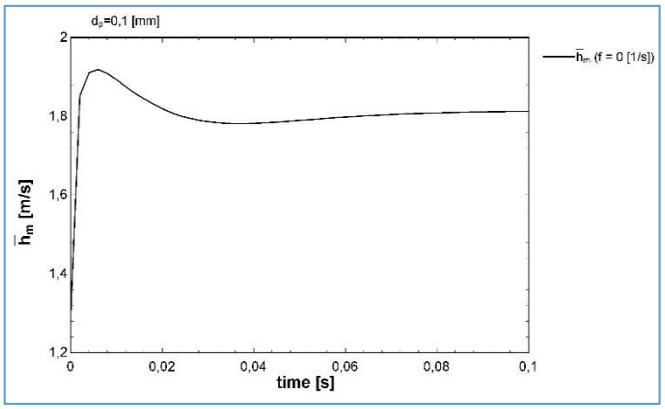

Fig. 5c: Mass transfer coefficient under steady flow.

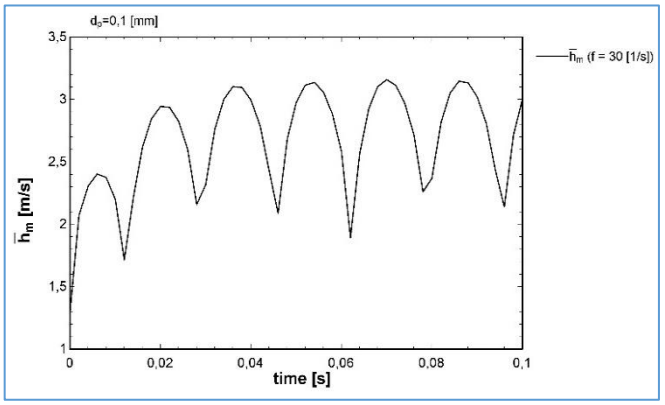

Fig. 5d: Mass transfer coefficient under pulsating flow.

Figures 6a and 6b shows the hydrodynamics of different particle sizes in acoustic field and in steady flow. Terminal velocity is attained only for the 0.1 mm particle size, in non-oscillating flow. The time to reach terminal velocity increases as particle size increases.

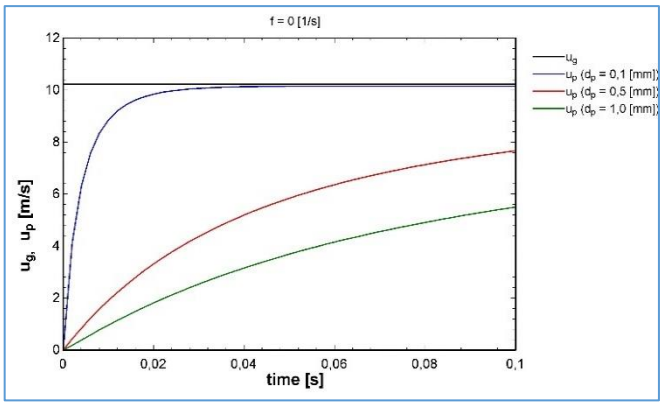

Fig. 6a: Steady gas and particle velocities as a function of time.

Figure 6b shows the gas and particle velocities under induced acoustic field. The 0.1 mm particle closely follows the gas alternating flow. Larger particles oscillate at much lower amplitudes and average velocities.

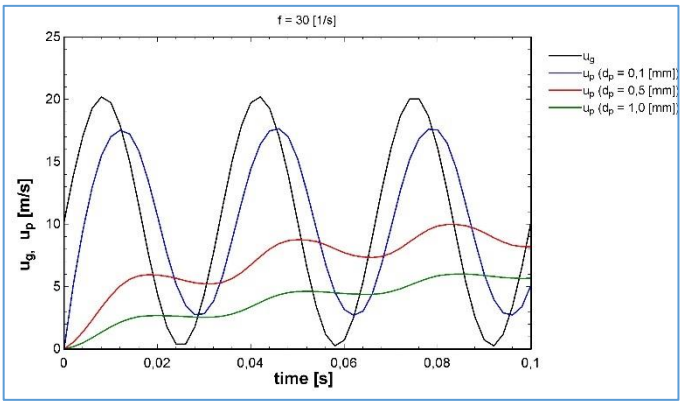

Fig. 6b: Oscillating gas and particle velocities as a function of time.

The temperature and moisture concentration fields experiences change due to acoustic flow, as noted in Fig. 7b and 7d, while exhibit different behavior for the situation without oscillation frequency in figures 7a and 7c.

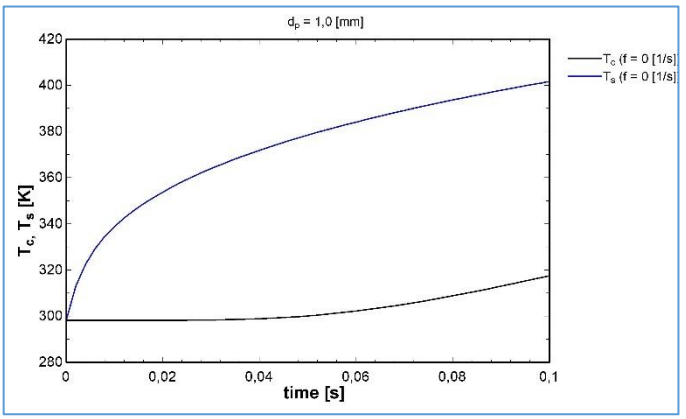

Fig. 7a: Temperature field as a function of time under steady flow.

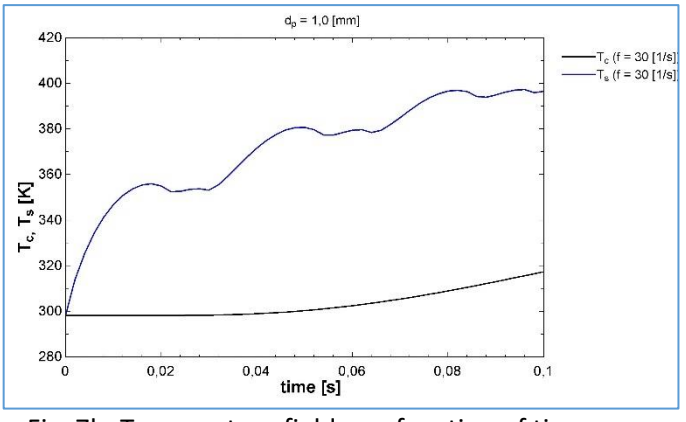

Fig. 7b: Temperature field as a function of time under pulsating flow.

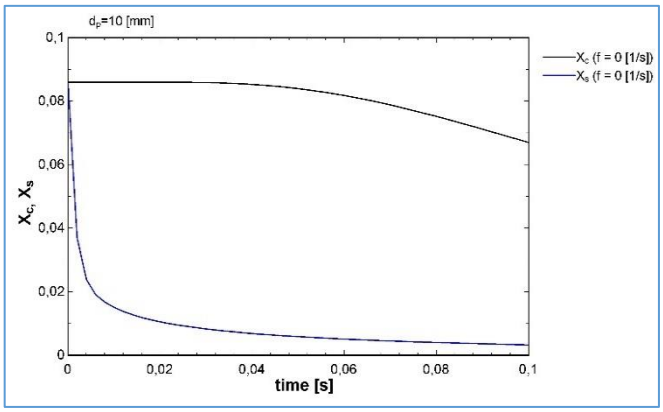

Fig. 7c: Moisture content field as a function of time under steady flow.

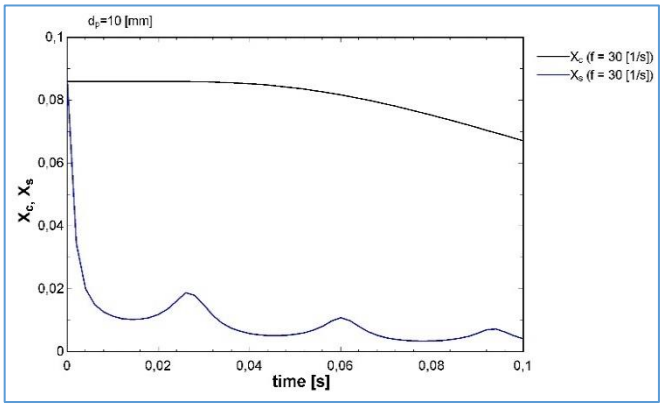

Fig. 7d: Moisture content field as a function of time under pulsating flow.

4.2 Conclusions

The developed model provides particles' hydrodynamic, temperature and moisture content simulation. In such manner, it is a valuable tool to study biomass drying.

Convective heat and mass transfer coefficients $\bar{h}$ and $\bar{h}_m$ increases by the presence of an acoustic field.

Reduced influence on velocity profile was observed for larger particle sizes (with diameter equal or higher than 0.5 mm).

The model allows further studies on the behavior of other feedstocks under the influence of acoustic field.

REFERENCE

[1] Cozzi L, Gould T. World Energy Outlook. International Energy Agency – 2021.

[2] Sharma A, Pareek V, Zhang D. Biomass Pyrolysis—A Review of Modelling, Process Parameters and Catalytic Studies. Renewable and Sustainable Energy Reviews, 50, 1081-1096. 2015.

[3] Downie, A. BEST Pyrolysis Technology: A Solution for the Greenhouse Challenge. BEST Energies, Australia. ThermalNet Newsl. 2007, 5, 5.

[4] Bridgewater, A. Biomass fast pyrolysis. Thermal Science.2004. 8. 21-50.

[5] PAUDEL, B.; FENG Z. G. Prediction of minimum fluidization velocity for binary mixtures of biomass and inert particles, Powder Technol, v. 237, p. 134-140, mar 237.

[6] AGU, C. E.; PFEIFER, C.; EIKELAND. M.; TOKHEIM, L.; MOLDESTAD, B. .M E. Measurement and Characterization of Biomass Mean Residence Time in an Air-Blown Bubbling Fluidized Bed Gasification Reactor, Fuel, v. 253 p. 1414-1423, oct 2019.

[7] Glass S, Zelinka, S. Moisture Relations and Physical Properties of Wood. p. 1–20, [2010]. Wood handbook – wood as an engineering material. General Technical Report FPL-GTR-282, Chapter 4. U.S. Department of Agriculture, Forest Service, Forest Products Laboratory.

[8] Scalet V, Santos L, Brasil R, Yamaji F. Caracterização de serragem de Eucalyptus sp. e de Pinus sp. para a produção de briquetes. Campinas: 2013. Accessed 15 May 2022. Available at: <https://proceedings.science/cbcm-2013/papers/caracterizacao-de-serragem-de-eucalyptus-sp-e-de-pinus-sp-para-a-producao-de-briquetes->

[9] Ikegwu UM, Ozonoh M, Daramola MO. Kinetic Study of the Isothermal Degradation of Pine Sawdust during Torrefaction Process. *ACS Omega*. 2021;6(16):10759-10769. Published 2021 Apr 14.

[10] Veras C, Carvalho J, Ferreira M. The Chemical Percolation Devolatilization Model Applied to the Devolatilization of Coal in High Intensity Acoustic Fields. Journal of the Brazilian Chemical Society, v. 13, n. 3, p. 358–367, Jun. 2002.

[11] Thibault J, Bergeron S, Bonin H. On finite-difference solutions of the heat equation in spherical coordinates. May, 1987.

[14] Ranz W, Marshall W. Evaporation from drops. Chemical Engineering Progress, 1952.

[13] Schwertz F. A., Brow, J. E. Diffusivity of Water Vapor in Some Common Gases. The Journal of Chemical Physics, v. 19, n. 5, p. 640–646, May, 1951.

[14] EES,2022. Engineering Equation Solver, F-Chart Software, accessed 8 April 2022. http://www.fchart.com/ees/.

[15] Nellis G, Klein S. Heat Transfer. 1st ed. New York: Cambridge; 2008.